Int. J. Heat Mass Transfer. Vol. 22, pp. 1657–1667.
Pergamon Press Ltd. 1979. Printed in Great Britain.

0017 9310/79/1201-1657 $02.00/0

SOLUTION OF RADIATION–CONDUCTION PROBLEMS WITH COLLOCATION METHOD USING B-SPLINES AS APPROXIMATING FUNCTIONS

T. C. CHAWLA and S. H. CHAN*

Reactor Analysis and Safety Division, Argonne National Laboratory, Argonne, IL 60439, U.S.A.

(*Received* 18 *January* 1979 *and in revised form* 18 *May* 1979)

Abstract – A collocation method employing B-splines as approximating functions and the Gaussian quadrature points as the collocation points is introduced for the first time to the solution of heat transfer problems governed by simultaneous conduction and radiation. It is demonstrated that this method provides an alternative noniterative technique which, with only a small number of equations, can produce solutions as accurate as the finite-difference method, and at a very reasonable computational cost. By comparison with exact analytical solution for the case of pure radiation, it is shown that, for up to moderate values of optical thickness, one needs to solve no more than 6 equations to obtain an accuracy better than 2%. The method with these characteristics appears to be an attractive candidate for the solution of radiation–conduction problems pertaining to LMFBR core disruptive meltdown accident analyses.

NOMENCLATURE

a_i,	coefficients of expansion;
d_j,	multiplicity at the interior breakpoints;
$g_k(s;\eta)$,	function defined by equation (15);
k,	order of B-splines;
l,	number of intervals;
m,	number of boundary conditions;
N_{cr},	conduction–radiation parameter defined by equation (4);
$N_{i,k}(\eta)$,	normalized B-splines defined by equation (16);
n,	the number of expansion coefficients;
p,	the number of collocation points per interval;
q_r,	radiation heat flux;
q_w,	total heat flux at the lower wall;
T,	temperature;
T_1,	temperature at the lower wall;
T_2,	temperature at the upper wall;
y,	dimensional coordinate from the lower wall.

Greek symbols

α_0,	$2[\sigma T^4(0) - T_2^4]/(T_1^4 - T_2^4)$;
β_0,	$2[\sigma T^4(\eta_0) - T_2^4]/(T_1^4 - T_2^4)$;
η,	nondimensional coordinate from the lower plate;
η_i,	breakpoints;
θ,	T/T_1;
κ,	absorption coefficient;
λ_j,	Gaussian–Legendre points in the interval $[-1, 1]$;
ν,	degree of smoothness at the interior breakpoints;
ξ,	dummy integration variable in equation (2);
ξ_i,	knots at the breakpoints;
σ,	Stefan–Boltzmann constant.

INTRODUCTION

IN HYPOTHETICAL core disruptive and meltdown accidents such as initiated by loss of flow in a liquid metal cooled fast breeder reactor (LMFBR), excessively high temperatures are encountered such that radiation can become a significant mode of heat transfer compared to conduction and convection. Recently, effort has been expended to investigate the effect of radiation heat transfer in some safety analyses [1–3]. However integral analyses of these postulated accidents require massive computer codes which can strain the capacity of even the largest of the computers available both with respect to storage and computing time requirements. Therefore, one of the desired requirements for including the effect of radiation heat transfer in accident analysis codes is that the computational method utilized be of high order so that the storage and computation time requirements are minimized. It is with this motivation that the application of the collocation method to radiation heat transfer problems is pursued in this paper.

It is well known that the formulation of the radiative heat transfer problem combined with the conduction mode of heat transfer leads to a nonlinear integro–differential equation. There are no general solutions available for this integro–differential equation because of inherent complexity resulting from the radiative contribution to the total heat flux for a given geometrical configuration of the system. Therefore, by necessity only finite-difference and approximate solutions for very specific geometrical configurations are available. Steady-state heat transfer by coupled conduction and radiation through a plane

* Energetics Department, The University of Wisconsin-Milwaukee, Milwaukee, WI 53201, U.S.A.

layer of an absorbing and emitting medium bounded by two opaque parallel walls has been studied most widely. Viskanta and Grosh [4, 5] solved iteratively the Fredholm nonlinear integral equation resulting from integrating the original integro–differential equation twice. Using the same technique, the nongray effects in the above geometry were studied by Crosbie and Viskanta [6] and Anderson and Viskanta [7]. There are, however, a number of other methods such as the exponential kernel approximation employed by Lick [8], the method of quasilinearization used by Timmons and Mingle [9], the combination of normal-mode expansion and an iterative technique employed by Lii and Ozisik [10], and the method in which the integro–differential equation is reduced to a nonlinear differential equation by a Taylor series expansion of the dependent variable occurring as the fourth power of temperature as used by Anderson and Viskanta [11]. An extensive review of the literature on heat transfer in semitransparent solids is presented by Viskanta and Anderson [12]. For the case of pure radiation in the above-mentioned plane geometry, both exact analytical and numerical solutions [13–15] are also available. The majority of the above studies have utilized numerical methods which are iterative in nature. Although the respective procedures underlying these iterative methods are quite straightforward, they are computationally very time-consuming and have large storage requirements. This is because of the iterations involved and the size of the system of finite-difference equations resulting from the choice of small step sizes necessary for producing desired accuracy, particularly for the case of an optically thick medium. This last limitation of finite-difference methods is particularly serious with regard to their application to LMFBR accident analysis codes because molten mixed oxide fuels of uranium and plutonium are optically thick.

An alternative method, based on collocation combined with the use of approximating subspaces, overcomes many of the above-described disadvantages of the iterative finite-difference methods by virtue of being a higher order and noniterative method requiring the solution of only a small number of equations to achieve the desired accuracy at a very reasonable computational cost. The method consists of expanding the unknown temperature profile in terms of a piecewise B-spline basis in the space variable. The unknown coefficients in the expansion are obtained by requiring that the resulting equation be satisfied at a number of points (in particular at the Gaussian quadrature points) in the field equal to the number of unknown coefficients. This collocation procedure reduces the integro–differential equation to a system of nonlinear algebraic equations which are solved by nonlinear system solvers based on various modifications and combinations of Newton's algorithm and the method of steepest descent.

Previously, for solving pure radiative transfer problems, the spline collocation method has been utilized by Kanasz and Hummer [16]. These authors used the smooth cubic splines with breakpoints as the collocation points. It has been shown, however, by Douglas and Dupont [17] and De Boor and Swartz [18] that the use of other than the optimum points as collocation points produces lower order accuracy. Similar to the above spline collocation method, but more accurate, is the method known as the Hermitian method developed by Auer [19] also for solving radiative problems.

DESCRIPTION OF THE PROBLEM

Since the purpose of the present paper is to demonstrate for the first time the applicability, versatility and the order of accuracy of the collocation method to combined radiation and conduction heat transfer problems, we have chosen a simple physical system which retains the essential features of radiative heat transfer but avoids the distractions of complex geometrical relationships. The physical system considered is shown in Fig. 1. We will assume that the medium is gray, nonscattering and at rest, and that the absorption coefficient and thermal conductivity of the medium are independent of temperature. The bounding surfaces consist of two parallel black plates which extend indefinitely in all directions and are isothermal but maintained at two different temperatures T_1 and T_2, respectively. That is, heat transfer by both modes under consideration is one-dimensional.

With the previously discussed assumptions, the equation expressing conservation of energy is given as [20]

$$K\kappa \frac{d^2T}{d\eta^2} = \frac{dq_r}{d\eta} \tag{1}$$

where K is the thermal conductivity of medium, T is the absolute temperature in °K, κ is the absorption coefficient, η is the optical depth defined as $\eta = \kappa y$, y being the coordinate from the lower plate. Here, q_r is the radiation heat flux given as [20]

$$\begin{aligned} q_r(\eta) = {} & 2\sigma T_1^4 E_3(\eta) - 2\sigma T_2^4 E_3(\eta_0 - \eta) \\ & + 2\int_0^{\eta} \sigma T^4(\xi) E_2(\eta - \xi)d\xi \\ & - 2\int_{\eta}^{\eta_0} \sigma T^4 E_2(\xi - \eta)d\xi. \end{aligned} \tag{2a}$$

The total heat flux at the lower wall, conductive plus radiative, is

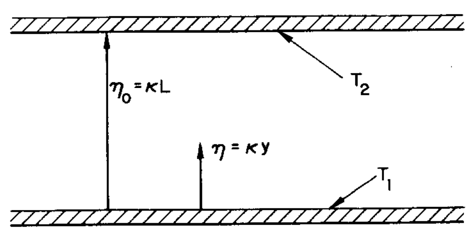

FIG. 1. One-dimensional combined conduction and radiation.

$$q_w = \left(-\kappa K\frac{\partial T}{\partial \eta} + q_r\right)_{\eta=0}. \quad (2b)$$

The derivative of heat flux $q_r(\eta)$ can be written as

$$\frac{dq_r}{d\eta} = -\left[2\sigma T_1^4 E_2(\eta) + 2\sigma T_2^4 E_2(\eta_0 - \eta) + 2\int_0^{\eta_0} \sigma T^4(\xi)E_1(|\eta - \xi|)d\xi - 4\sigma T^4(\eta)\right]. \quad (3)$$

Here, the $E_n(\xi)$ are the exponential integral functions and η_0 is the optical thickness of the medium.

It is convenient to nondimensionalize the above equations by introducing the following dimensionless quantities:

$$\theta(\eta) = \frac{T(\eta)}{T_R},\ \theta_1 = \frac{T_1}{T_R},\ \theta_2 = \frac{T_2}{T_R},\ N_{cr} = \frac{K\kappa}{4\sigma T_R^3} \quad (4)$$

where T_R is an arbitrary temperature.

With the use of the above nondimensional quantities, and of equation (3) into equation (1), we obtain

$$N_{cr}\frac{d^2\theta}{d\eta^2} - \theta^4(\eta) + \frac{1}{2}\left[\theta_1^4 E_2(\eta) + \theta_2^4 E_2(\eta_0 - \eta) + \int_0^{\eta_0} \theta^4(\xi)E_1(|\eta - \xi|)d\xi\right] = 0. \quad (5)$$

Expression (2) takes the form

$$q_r^* = \frac{q_r}{\sigma T_R^4} = \left[2\theta_1^4 E_3(\eta) - \theta_2^4 E_3(\eta_0 - \eta) + \int_0^{\eta} \theta^4(\xi)E_2(\eta - \xi)d\xi - \int_{\eta}^{\eta_0} \theta^4(\xi)E_2(\xi - \eta)d\xi\right]. \quad (6a)$$

The total heat flux q_w given by expression (2b) in dimensionless notation becomes

$$q_w^* = \frac{q_w}{\sigma T_R^4} = -4N_{cr}\frac{d\theta}{d\eta} + \theta_1^4 - \left[2\theta_2^4 E_3(\eta_0) + \int_0^{\eta_0} \theta^4(\xi)E_2(\xi)d\xi\right]. \quad (6b)$$

The boundary conditions that equation (5) must satisfy are

$$\theta(0) = \theta_1, \quad \theta(\eta_0) = \theta_2. \quad (7)$$

Clearly the integro-differential equation (5) is nonlinear because temperature $\theta(\eta)$ occurs to the fourth power in terms depicting the effect of radiation. The parameter N_{cr} occurring in this equation is called the conduction–radiation parameter and determines the relative role of the conduction vs radiation term. For large values of N_{cr}, conduction predominates, and at low values of N_{cr}, radiation is the dominant mode of heat transfer. We may note specifically as $N_{cr} \to 0$, equation (5) reduces to an integral equation, in which case the boundary conditions (7) must be dropped; consequently, 'temperature slip' at the bounding surfaces will occur.

METHOD

We shall assume that $\theta(\eta)$ can be approximated by nonsmooth piecewise polynomials in η generated by B-spline basis sets. More specifically, let the interval $[0, \eta_0]$ be subdivided by a set of points, called the breakpoints, thus

$$\pi: 0 = \eta_1 < \eta_2 < \ldots < \eta_l < \eta_{l+1} = \eta_0.$$

Relative to this partition π, let $\mathscr{P}_{k,\pi,v}$ denote the space of piecewise polynomials $\{f_i\}_{i=1}^l$ of order k (degree $= k - 1$) and smoothness $\bar{v} = \{v_i\}_{i=2}^l$ (i.e. continuity of derivatives of functions f_i up to order $v_i - 1$) at the interior breakpoints. So

$$\dim \mathscr{P}_{k,\pi,v} = n = kl - \sum_{i=2}^{l} v_i, \quad (8)$$

where the first term represents the total number of coefficients of l piecewise polynomials (one per interval of the partition π) and the second term represents the total number of smoothness constraints to be imposed on functions $\{f_i\}_{i=1}^l$ at the interior points. Now, let the approximating subspace $\mathscr{S}_{k,\pi,v} \subset \mathscr{P}_{k,\pi,v}$ be obtained by imposing m boundary conditions on the elements in $\mathscr{P}_{k,\pi,v}$, then

$$\dim \mathscr{S}_{k,\pi,v} = kl - \sum_{i=2}^{l} v_i - m. \quad (9)$$

We now seek an approximate solution of equation (5) of the form

$$\theta(\eta) = \sum_{i=1}^{n} a_i w_i(\eta) \quad (10)$$

where the set $\{w_i(\eta)\}_{i=1}^n$ forms a basis for the approximating subspace $\mathscr{S}_{k,\pi,v}$ of functions which satisfy boundary conditions (7). The expansion (10) is then used in equation (5) and this equation is required to hold at a specified set of (collocation) points. This process leads to a system of nonlinear algebraic equations for the coefficients $\{a_i\}_{i=1}^n$. Now let p be the number of collocation points selected per interval in partition π, then we must have

$$\dim \mathscr{S}_{k,\pi,v} = pl. \quad (11)$$

Thus, we obtain from equations (9) and (11)

$$pl \equiv kl - \sum_{i=2}^{l} v_i - m. \quad (12)$$

If we require that $v_i = v$ at each of the interior breakpoints, identity (12) becomes

$$pl \equiv kl - v(l-1) - m \equiv (k-v)l + (v-m) \quad (13)$$

which must hold for any number of subintervals l; thus

$$k = p + v, \quad v = m, \quad n = pl + v. \quad (14)$$

The above procedure and the discussion of the B-splines to be given below will be well illustrated subsequently by considering very specific examples.

B-spline basis

A very detailed discussion of B-splines basis is given in Refs. [21] and [22]. In the latter reference a discussion of an algorithm for generating these splines is also given. For use in the present analysis, we summarize below some of the important features of B-splines.

To generate a B-spline basis for the space $\mathscr{P}_{k,\pi,\nu}$, define

$$g_k(s;\eta) = (s-\eta)_+^{k-1} = \begin{cases}(s-\eta)^{k-1} & s \geqslant \eta \\ 0 & s < \eta\end{cases} \quad (15)$$

and let the set of multiple knots $\{\xi_i\}_{i=1}^{n+k}$ be defined by

$$\xi_1 = \ldots = \xi_k = \eta_1,$$

$$\xi_{k+1} = \ldots = \xi_{k+d_2} = \eta_2,$$

$$\vdots$$

$$\xi_{k+d_2+\ldots+d_{j-1}+1} = \ldots = \xi_{k+d_2+\ldots+d_j} = \eta_j, \quad j \leqslant l,$$

$$\vdots$$

$$\xi_{n+1} = \ldots = \xi_{n+k} = \eta_{l+1}.$$

The first and last breakpoints, η_1 and η_{l+1}, have multiplicity k and the interior breakpoints have multiplicity $d_j = k - \nu_j$. The construction of these knots is shown schematically in Fig. 2. With each knot, we associate the normalized B-spline $N_{i,k}(\eta)$ defined as the kth divided difference of $g_k(s,\eta)$ in s on the set of knots $\xi_1, \ldots, \xi_{i+k}$, i.e.

$$\begin{aligned} N_{i,k}(\eta) &= (\xi_{i+k} - \xi_i) g_k(\xi_i, \ldots, \xi_{i+k};\eta) \\ &= g_k(\xi_{i+1}, \ldots, \xi_{i+k};\eta) \\ &\quad - g_k(\xi_i, \ldots, \xi_{i+k-1};\eta). \end{aligned} \quad (16)$$

Thus, from equations (15) and (16), we have

$$N_{i,k}(\eta) = 0 \quad \text{for} \quad \eta \notin [\xi_i, \xi_{i+k}], \quad (17)$$

which implies that $N_{i,k}(\eta)$ has its support in $[\xi_i, \xi_{i+k}]$. In addition the normalized B-splines $N_{i,k}(\eta)$ possess the following useful properties:

$$\sum_{i=1}^{n} N_{i,k}(\eta) \equiv 1, \quad (18)$$

$$N_{i,k}(\eta) > 0 \quad \text{for} \quad \eta \in (\xi_i, \xi_{i+k}), \quad (19)$$

$$N_{1,k}(\eta_1) = 1, \quad N'_{1,k}(\eta_1) = -(k-1)/(\eta_2 - \eta_1), \quad (20)$$

$$N_{n,k}(\eta_{l+1}) = 1, \quad N'_{n,k}(\eta_{l+1}) = (k-1)/(\eta_{l+1} - \eta_l). \quad (21)$$

Since $N_{i,k}(\eta) \geqslant 0$ for $1 \leqslant i \leqslant n$ and $\eta \in [\eta_1, \eta_{l+1}]$, it follows from normalization property (18) that

$$N_{i,k}(\eta_1) = 0 \quad \text{for} \quad 1 < i \leqslant n,$$

$$N_{i,k}(\eta_{l+1}) = 0 \quad \text{for} \quad 1 \leqslant i < n. \quad (22a,b)$$

For the values of the derivatives of $N_{i,k}(\eta)$ at the end breakpoints, we start by considering the behavior of $N_{i,k}(\eta)$ at $\eta = \eta_1$ for $2 < i \leqslant n$. Let us first consider the case $k+1 \leqslant i \leqslant n$: since $N_{i,k}(\eta)$ has its support in (ξ_i, ξ_{i+k}) with $\xi_i \geqslant \eta_2$, it follows that $N_{i,k}(\eta) \equiv 0$ for $\eta < \eta_2$; thus $N_{i,k}(\eta)$ and all its derivatives will vanish at $\eta = \eta_1$. Next, we consider $2 < i \leqslant k$, and in particular the case $i = 3$: since $N_{3,k}(\eta)$ is a kth divided difference over the set $\xi_3, \ldots, \xi_{k+3}$, where $\xi_3 = \ldots = \xi_k (= \eta_1)$ appear $k-2$ times, this divided difference $N_{3,k}(\eta)$ has a knot of multiplicity $d = k-2$ at $\eta = \eta_1$; since the smoothness index ν for $N_{3,k}(\eta)$ at η_1 satisfies the relation $\nu = k - d = k - (k-2) = 2$, we see that $N_{3,k}(\eta)$ has a continuous derivative at $\eta = \eta_1$. Now $N_{3,k}(\eta) \equiv 0$ for $\eta < \eta_1$; therefore $N'_{3,k}(\eta_1) = 0$. When $3 < i \leqslant k$, a similar argument shows that $N_{i,k}(\eta)$ has $i-2$ continuous derivatives at $\eta = \eta_1$, thus $N'_{i,k}(\eta_1) = 0$ for $2 < i \leqslant k$. More generally, we have

$$N_{i,k}^{(q)}(\eta_1) = 0 \quad \text{for } 0 \leqslant q \leqslant i-2 \quad \text{and } 2 \leqslant i \leqslant k. \quad (23)$$

Here we have used equation (22a) for the case $i = 2$. From the normalization property (18) we have

$$\sum_{i=1}^{n} N'_{i,k}(\eta) \equiv 0 \quad \text{for} \quad \eta \in [\eta_1, \eta_{l+1}]. \quad (24)$$

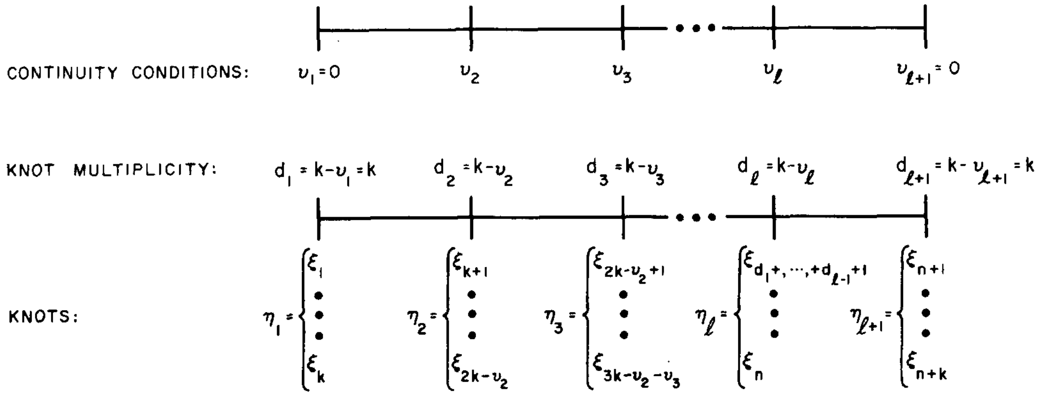

FIG. 2. Construction of knots at various breakpoints.

The use of equation (23) in equation (24) gives

$$N'_{1,k}(\eta_1) + N'_{2,k}(\eta_1) = 0 \quad (25)$$

with $N'_{1,k}(\eta_1)$ given by equation (20). Analogous argument will show that

$$N^{(q)}_{i,k}(\eta_{l+1}) = 0 \quad \text{for } 0 \leqslant q \leqslant n-i-1$$
$$\text{and } n-k+1 \leqslant i \leqslant n-1. \quad (26)$$

Thus, from equations (24) and (26), we obtain

$$N'_{n-1,k}(\eta_{l+1}) + N'_{n,k}(\eta_{l+1}) = 0 \quad (27)$$

with $N'_{n,k}(\eta_{l+1})$ given by equation (21).

Expansions in normalized B-splines

Expansion (10) for $\theta(\eta)$ in terms of normalized B-splines becomes

$$\theta(\eta) = \sum_{i=1}^{n} a_i N_{i,k}(\eta). \quad (28a)$$

Since each $N_{i,k}(\eta)$ is nonzero only in the interval $\eta \in [\xi_i, \xi_{i+k}]$, it follows that when $\eta \in (\eta_j, \eta_{j+1})$, $N_{i,k}(\eta) \neq 0$ for $i = J-k+1, \ldots, J$ with $J = j(k-v)+v$ for $1 \leqslant j \leqslant l$. So equation (28a) becomes

$$\theta(\eta) = \sum_{i=J_L}^{J} a_i N_{i,k}(\eta),$$
$$\text{for } \eta \in (\eta_j, \eta_{j+1}), \quad 1 \leqslant j \leqslant l \quad (28b)$$

where $J_L = J-k+1$.

In application to equation (5), we observe that two boundary conditions given by equation (7) are imposed, so that $m = v = 2$ in equation (14). Thus we will be concerned with normalized B-splines of order $k = p+2$. The substitution of equation (28) into equation (5) yields

$$N_{cr} \sum_i a_i N''_{i,k}(\eta) - \left[\sum_i a_i N_{i,k}(\eta)\right]^4 + \frac{1}{2}\left\{\theta_1^4 E_2(\eta) + \theta_2^4 E_2(\eta_0 - \eta) + \int_0^{\eta_0}\left[\sum_i a_i N_{i,k}(\xi)\right]^4 E_1(|\eta-\xi|)\mathrm{d}\xi\right\} = 0 \quad (29)$$

and the use of equations (20), (21) and (22) in equation (7) yields

$$a_1 = \theta_1, \quad a_n = \theta_2. \quad (30)$$

With $a_1 = \theta_1$ and $a_n = \theta_2$, equation (29) contains $n-2$ unknown coefficients. To determine these unknown coefficients, we require that equation (29) be satisfied at $n-2 = pl$ collocation points. This set of pl equations provides a set of $n-2$ nonlinear algebraic equations for $n-2$ unknown coefficients. In accordance with the approximation theory [17, 18], the Gaussian–Legendre quadrature points of order p relative to the interval $[\eta_i, \eta_{i+1}]$ are chosen as the collocation points in each subinterval. If, for each integer p, $-1 < \lambda_1 < \lambda_2 < \ldots < \lambda_p < 1$ denote the p Gaussian–Legendre points relative to the interval $[-1, 1]$, then the p collocation points in each subinterval $[\eta_i, \eta_{i+1}]$ are given as

$$\sigma_{i,j} = \tfrac{1}{2}(\eta_i + \eta_{i+1}) + \tfrac{1}{2}\lambda_j(\eta_{i+1} - \eta_i),$$
$$1 \leqslant j \leqslant p, \quad 1 \leqslant i \leqslant l. \quad (31a)$$

The linear index for these collocation points may be generated by setting

$$\gamma_{(i-1)p+j} = \sigma_{i,j} \quad \text{for } 1 \leqslant j \leqslant p \text{ and } 1 \leqslant i \leqslant l. \quad (31b)$$

Evaluating equation (29) at the collocation points $\sigma_{i,j}$, we obtain the following system of equations:

$$N_{cr} \sum_{i=J_L}^{J} a_i N''_{i,k}(\sigma_{q,j}) - \left[\sum_{i=J_L}^{J} a_i N_{i,k}(\sigma_{q,j})\right]^4 + \frac{1}{2}\left\{\theta_1^4 E_2(\sigma_{q,j}) + \theta_2^4 E_2(\eta_0 - \sigma_{q,j}) + \int_0^{\eta_0}\left[\sum_{i=J_L}^{J} a_i N_{i,k}(\sigma_{q,j})\right]^4 E_1(|\sigma_{q,j} - \xi|)\mathrm{d}\xi\right\} = 0 \quad (32)$$

wherein

$$\eta = \sigma_{q,j} \in (\eta_q, \eta_{q+1}), \quad J = q(k-2)+2,$$
$$1 \leqslant q \leqslant l, \quad 1 \leqslant j \leqslant p. \quad (33)$$

An illustrative example

For the purpose of illustrating the application, we consider a specific calculation in which $l = 3$, $\eta_0 = 1$. With two boundary conditions given by equation (7), we clearly have $m = 2$ and $v = m = 2$ in equation (14). If we choose $p = 2$, then we obtain $k = 4$ and $n = 8$ from equation (14). For the above values of various parameters, namely $k = 4$, $v = 2$, $l = 3$, and the breakpoints at $\eta = 0, 0.3, 0.7$ and 1.0, Fig. 3 shows the plot of both B-splines and their corresponding first derivatives calculated by using the subroutine package developed by De Boor [22]. From this figure it is clear that in every interval there are only four B-spline basis functions that are nonzero. This can also be seen by considering expansion (28) in each interval separately. Thus, for $j = 1$, $\eta \in (\eta_1, \eta_2)$,

$$\theta(\eta) = \sum_{i=1}^{4} a_i N_{i,k}(\eta) \quad (34a)$$

wherein $J = j(k-v)+v = 4$, $J_L = J-k+1 = 1$; for $j = 2$, $\eta \in (\eta_2, \eta_3)$,

$$\theta(\eta) = \sum_{i=3}^{6} a_i N_{i,k}(\eta); \quad (34b)$$

for $j = 3$, $\eta \in (\eta_3, \eta_4)$,

$$\theta(\eta) = \sum_{i=5}^{8} a_i N_{i,k}(\eta). \quad (34c)$$

For $p = 2$, λ_j in equation (31a) has the values $\lambda_1 = -1/\sqrt{3}$ and $\lambda_2 = 1/\sqrt{3}$. With these values of λ_j, we can readily calculate collocation points from equation

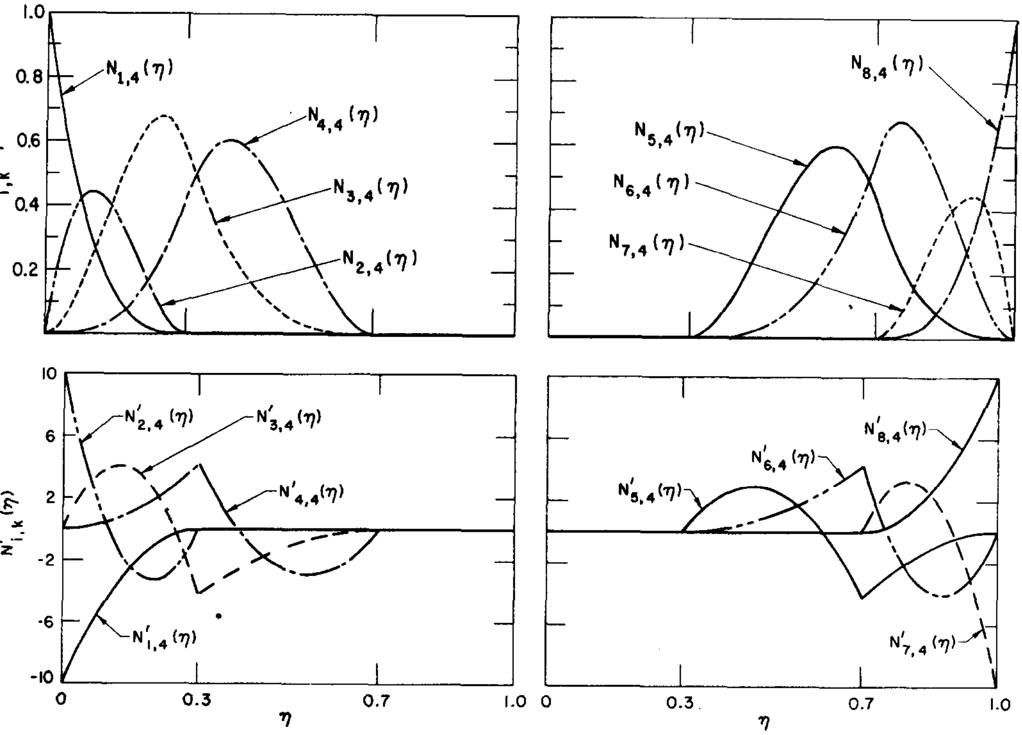

FIG. 3. Plots of B-splines $N_{i,k}(\eta)$ and first derivative $N'_{i,k}(\eta)$ for $k = 4$, $v = 2$ and $l = 3$ with breakpoints at $\eta = 0, 0.3, 0.7$ and 1.

(31) by using the previously given break-points. In view of expansion (34), equation (32) yields the following set of six equations:

for $q = 1$ and $1 \leqslant j \leqslant 2$,

$$N_{cr} \sum_{i=1}^{4} a_i N''_{i,k}(\sigma_{1,j}) - \left[\sum_{i=1}^{4} a_i N_{i,k}(\sigma_{1,j})\right]^4 + \frac{1}{2}\left\{\theta_1^4 E_2(\sigma_{1,j}) + \theta_2^4 E_2(\eta_0 - \sigma_{1,j}) + \int_0^{\eta_0} \left[\sum_{i=1}^{4} a_i N_{i,k}(\sigma_{1,j})\right]^4 E_1(|\sigma_{1,j} - \xi|)\mathrm{d}\xi\right\} = 0; \quad (35a)$$

for $q = 2$ and $1 \leqslant j \leqslant 2$,

$$N_{cr} \sum_{i=3}^{6} a_i N''_{i,k}(\sigma_{2,j}) - \left[\sum_{i=3}^{6} a_i N_{i,k}(\sigma_{2,j})\right]^4 + \frac{1}{2}\left\{\theta_1^4 E_2(\sigma_{2,j}) + \theta_2^4 E_2(\eta_0 - \sigma_{2,j}) + \int_0^{\eta_0} \left[\sum_{i=3}^{6} a_i N_{i,k}(\sigma_{2,j})\right]^4 E_1(|\sigma_{2,j} - \xi|)\mathrm{d}\xi\right\} = 0; \quad (35b)$$

for $q = 3$ and $1 \leqslant j \leqslant 2$,

$$N_{cr} \sum_{i=5}^{8} a_i N''_{i,k}(\sigma_{3,j}) - \left[\sum_{i=5}^{8} a_i N_{i,k}(\sigma_{3,j})\right]^4 + \frac{1}{2}\left\{\theta_1^4 E_2(\sigma_{3,j}) + \theta_2^4 E_2(\eta_0 - \sigma_{3,j}) + \int_0^{\eta_0} \left[\sum_{i=5}^{8} a_i N_{i,k}(\sigma_{3,j})\right]^4 E_1(|\sigma_{3,j} - \xi|)\mathrm{d}\xi\right\} = 0. \quad (35c)$$

The remaining two unknowns are determined by using equation (30). Thus, equations (35) and (30) constitute a set of eight equations to determine $n = 8$ unknowns.

COMPUTATIONAL DETAILS AND RESULTS

With a_1 and a_n given by equation (30), equation (32) constitutes a set of $n-2$ nonlinear algebraic equations which is solved by a library subroutine HYBRD1 [23] based upon a modification of the Powell hybrid method [24]. However the kernel $E_1(|\eta - \xi|)$ occurring in equation (5) or (32) is singular at $\xi = \eta$, therefore the evaluation of the integral in equation (32) is carried out by adaptive quadrature routine called DCADRE which is based upon a cautious adaptive Romberg extrapolation algorithm devised by De Boor [25]. The integrand evaluation is carried out by using cubic Hermite splines [26] for interpolation of temperature θ and the point values of exponential integral E_1 by library subroutine ESUBN, which uses rational Chebyshev approximations devised by Cody and Thacher [27]. We may note that the use of Hermite splines with its simple explicit basis is more convenient for the purposes of rapid interpolation. The relative error for evaluation of the integral in equation (32) was set at 10^{-5}, which in most cases permitted results to be computed by subroutine DCADRE with an estimated bound on the absolute error of less than 10^{-6}. The tolerance for nonlinear solver HYBRD1 was set at 10^{-7}. The algorithm converges if either the Euclidean norm of the residue vector of the set of equations (32) is at this tolerance, or if the algorithm estimates that the relative error is at or less than this tolerance.

From the previous discussion of the problem and the method of collocation based on the use of B-splines, we can identify the following sets of factors that affect the accuracy of the approximate solution: (i) optical thickness η_0, θ_2 and θ_1, conduction–radiation parameter N_{cr}, (ii) the distribution of breakpoints, (iii) the number of breakpoints, and (iv) the order of B-splines. The set (i) is particular to the conduction–radiation problem and is not part of a numerical procedure utilized, but has a considerable effect on the accuracy obtainable from the use of a given numerical procedure. The effect of the distribution of breakpoints can substantially influence the accuracy obtainable from 'boundary layer' type problems, however, for the range of parameters of set (i) investigated, it was felt the distribution of breakpoints would not significantly influence the accuracy obtainable and therefore uniform distribution of breakpoints was utilized throughout the study. For a fixed number of unknowns, it has been found previously [21] that the use of high order B-splines produces oscillations in the spatial distribution of temperature. These oscillations increase as the order of B-splines increases and hence as the number of intervals decreases. Furthermore, it has been demonstrated [17] that for a parabolic equation the use of cubic piecewise polynomials together with Gaussian quadrature points as collocation points results in an accuracy of up to fourth order. For this reason, we have kept the order of B-splines fixed at $k = 4$ throughout this study. As is well known for any finite-difference procedure, the number of breakpoints should have a considerable influence on the accuracy obtainable and the corresponding computational time, consequently these were varied from a value of $l = 2$ to $l = 30$.

For the purpose of comparing the accuracy of the solution by the collocation method, a well known, finite-difference solution based on the method discussed previously by Viskanta and Grosh [4, 6] was utilized. Unfortunately, the computational details, such as step size or the number of steps utilized, are not available. Therefore, the comparison is limited to checking the accuracy obtained by the method of collocation. However, the previous studies [21, 26] of this method in relation to the solution of conduction dominated heat transfer problems have demonstrated that the collocation method is far more accurate and faster than the usual finite-difference methods for these problems. The temperature at the lower wall was used for nondimensionalizing the temperature, therefore θ_1 was set at 1.0 for all runs, the value of θ_2 was left as a variable parameter. The specific values of parameters η_0, θ_2 and N_{cr} selected are the sample values chosen from Crosbie and Viskanta [6] and Viskanta and Grosh [4].

The solution of equation (32) is presented in Fig. 4 and Table 1. Figure 4 compares the temperature profiles as obtained by the collocation method for $l = 10$ with the Viskanta and Grosh [4] solution. As can be seen, there is very satisfactory agreement between the two results as the two solutions almost lie over each other. Table 1 gives the numerical comparison for the values of heat flux at the lower wall with the numerical

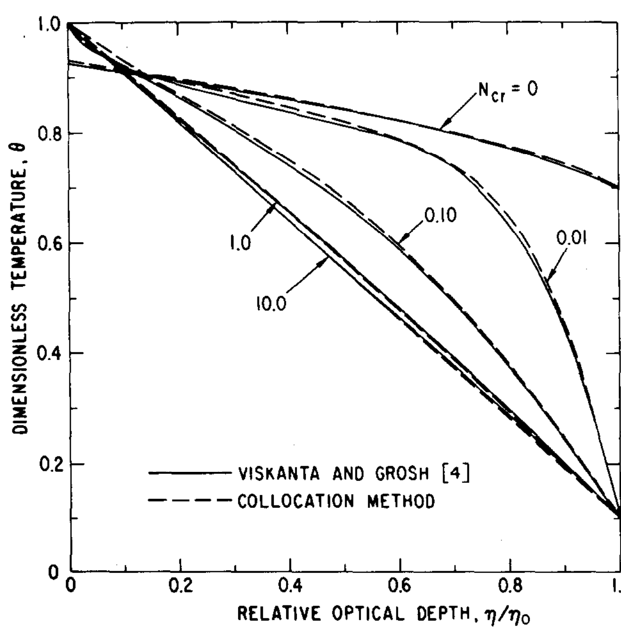

FIG. 4. Comparison of the temperature distribution obtained with collocation method for $l = 10$, with the finite-difference solution by Viskanta and Grosh [4] for $\theta_2 = 0.1$ and $\eta_0 = 1.0$.

Table 1. A comparison of collocation method with Crosbie and Viskanta's [6] finite difference solution

Optical thickness η_0	Plate-temperature ratio θ_2	Conduction-radiation parameter N_{cr}	Crosbie & Viskanta [6] numerical solution $q/\sigma T_1^4$	Collocation method, $q/\sigma T_1^4$						Heaslet & Warming exact solution $q_r/\sigma T_1^4$
				$l = 2$	$l = 5$	$l = 8$	$l = 10$	$l = 20$	$l = 30$	
				CPU = 18 s	CPU = 64 s	CPU = 142 s	CPU = 208 s			
		0	0.8585 (—)	0.8585 (—)	0.8585 (—)	0.8585 (—)	0.8585 (—)	0.8585 (—)		0.8585
		0.01	1.0799 (—)	1.0797 (—)	1.0799 (—)	1.0799 (—)	1.0799 (—)	1.0799 (—)		
0.1	0.5	0.1	2.8799 (—)	2.8799 (—)	2.8799 (—)	2.8799 (—)	2.8799 (—)	2.8799 (—)		
		1	20.8799 (—)	20.8799 (—)	20.8799 (—)	20.8799 (—)	20.8799 (—)	20.8799 (—)		
		10	200.8799 (—)	200.8799 (—)	200.8799 (—)	200.8799 (—)	200.8799 (—)	200.8799 (—)		
				CPU = 26 s	CPU = 87 s	CPU = 187 s	CPU = 274 s			
		0	0.5188 (—)	0.5185 (0.04%)	0.5188 (0.02%)	0.5188 (—)	0.5187 (—)	0.5187 (—)		0.5186
		0.01	0.5675 (—)	0.5478 (3.5%)	0.5657 (0.3%)	0.5671 (0.07%)	0.5673 (0.04%)	0.5675 (—)		
1.0	0.5	0.1	0.7694 (—)	0.7649 (0.6%)	0.7693 (0.0%)	0.7694 (—)	0.7694 (—)	0.7694 (—)		
		1	2.5724 (—)	2.5705 (0.07%)	2.5723 (0.007%)	2.5725 (—)	2.5725 (—)	2.5725 (—)		
		10	20.5723 (—)	20.5707 (0.008%)	20.5724 (—)	20.5724 (—)	20.5724 (—)	20.5724 (—)		
				CPU = 59 s	CPU = 193 s	CPU = 396 s	CPU = 515 s			
		0	0.1095 (—)	0.1020 (6.85%)	0.1094 (0.09%)	0.1097 (0.18%)	0.1097 (0.18%)	0.1096 (0.1%)	0.1095 (—)	0.1094 (Asymptotic solution for optically thick limit)
		0.01	0.1131 (0.5%)	0.0321 (71.0%)	0.1011 (10.0%)	0.1081 (3.9%)	0.1096 (2.6%)	0.1124 (0.09%)	0.1125 (—)	
10	0.5	0.1	0.1335 (—)	0.0978 (27.0%)	0.1258 (5.7%)	0.1308 (1.95%)	0.1319 (1.12%)	0.1329 (0.37%)	0.1334 (—)	
		1	0.3150 (—)	0.2832 (10.0%)	0.3101 (1.5%)	0.3136 (0.41%)	0.3142 (0.22%)	0.3149 (—)	0.3149 (—)	
		10	2.1146 (—)	2.0812 (1.58%)	2.1105 (0.19%)	2.1135 (0.05%)	2.1140 (0.03%)	2.1145 (0.005%)	2.1146 (—)	

Table 2. A comparison of collocation method with Heaslet and Warming's [14] exact solution for the case of heat transfer by radiation alone

Optical thickness η_0	$\alpha_0 = 2[T^4(0) - T_2^4]/(T_1^4 - T_2^4)$ Heaslet & Warming exact	Collocation method $l = 10$ CPU = 855 s	$l = 8$ CPU = 592 s	$l = 5$ CPU = 291 s	$l = 2$ CPU = 91 s	$\beta_0 = 2(T^4(\eta_0) - T_2^4)/(T_1^4 - T_2^4)$ Heaslet & Warming exact	Collocation method $l = 10$	$l = 8$	$l = 5$	$l = 2$	$q_r/\sigma(T_1^4 - T_2^4)$ Heaslet & Warming exact	Collocation method $l = 10$	$l = 8$	$l = 5$	$l = 2$
0.1	1.1419	1.1420 0.01%	1.1420 0.01%	1.1420 0.01%	1.1420 0.01%	0.8581	0.8580 0.01%	0.8580 0.01%	0.8580 0.01%	0.8580 0.01%	0.9157	0.9157 —	0.9157 —	0.9157 —	0.9157 —
0.2	1.2228	1.2229 0.005%	1.2229 0.005%	1.2229 0.005%	1.2229 0.005%	0.7772	0.7771 0.008%	0.7771 0.008%	0.7771 0.008%	0.7771 0.008%	0.8491	0.8492 0.009%	0.8492 0.009%	0.8492 0.009%	0.8492 0.009%
0.3	1.2838	1.2838 —	1.2838 —	1.2838 —	1.2839 0.007%	0.7162	0.7162 —	0.7162 —	0.7162 —	0.7162 —	0.7934	0.7936 0.02%	0.7936 0.02%	0.7936 0.02%	0.7936 0.02%
0.4	1.3331	1.3332 0.007%	1.3332 0.007%	1.3332 0.007%	1.3333 0.01%	0.6669	0.6668 0.01%	0.6668 0.01%	0.6668 0.01%	0.6669 —	0.7458	0.7458 —	0.7458 —	0.7459 0.007%	0.7458 —
0.5	1.3746	1.3747 0.004%	1.3747 0.004%	1.3747 0.004%	1.3748 0.01%	0.6254	0.6253 0.009%	0.6253 0.009%	0.6254 —	0.6254 —	0.7040	0.7041 0.01%	0.7042 0.02%	0.7042 0.02%	0.7041 0.01%
0.6	1.4103	1.4103 —	1.4103 —	1.4103 —	1.4105 0.02%	0.5897	0.5897 —	0.5897 —	0.5897 —	0.5898 0.02%	0.6672	0.6672 —	0.6673 0.02%	0.6673 0.02%	0.6672 —
0.8	1.4692	1.4692 —	1.4692 —	1.4692 —	1.4695 0.02%	0.5308	0.5308 —	0.5308 —	0.5309 0.01%	0.5311 0.05%	0.6046	0.6048 0.02%	0.6048 0.02%	0.6048 0.02%	0.6045 0.02%
1.0	1.5163	1.5163 —	1.5163 —	1.5163 —	1.5168 0.03%	0.4837	0.4837 —	0.4837 —	0.4838 0.02%	0.4842 0.1%	0.5532	0.5533 0.01%	0.5534 0.04%	0.5534 0.04%	0.5530 0.03%
1.5	1.6024	1.6024 —	1.6024 —	1.6024 —	1.6034 0.06%	0.3976	0.3977 0.02%	0.3977 0.02%	0.3978 0.05%	0.3987 0.3%	0.4572	0.4573 0.03%	0.4574 0.03%	0.4573 0.03%	0.4565 0.2%
2.0	1.6615	1.6616 0.003%	1.6615 —	1.6616 0.003%	1.6632 0.1%	0.3385	0.3385 —	0.3385 —	0.3387 0.07%	0.3403 0.5%	0.3900	0.3901 0.03%	0.3901 0.03%	0.3901 0.03%	0.3886 0.4%
2.5	1.7051	1.7051 —	1.7051 —	1.7052 0.005%	1.7075 0.1%	0.2949	0.2950 0.03%	0.2950 0.03%	0.2953 0.02%	0.2977 1.0%	0.3401	0.3402 0.04%	0.3402 0.04%	0.3402 0.03%	0.3379 0.6%
3.0	1.7386	1.7386 —	1.7386 —	1.7387 0.007%	1.7418 0.2%	0.2614	0.2615 0.04%	0.2616 0.08%	0.2620 0.2%	0.2653 1.5%	0.3016	0.3017 0.04%	0.3017 0.04%	0.3017 0.02%	0.2986 1.0%

data of Crosbie and Viskanta [6]. To establish the convergence, the number of intervals l was varied from 2 to 30 (or the value of n from 6 to 62). For small to moderate values of the optical thickness, $l = 20$ was adequate to obtain stability in the solution up to four decimal points. This was sufficiently accurate since the available finite-difference solution is given only to four decimal places. However, for the case of large optical thickness, e.g. $\eta_0 = 10$, higher values of l were necessary to achieve stability in the fourth decimal place. In the former case $l = 20$ was selected as the benchmark calculation and in the latter case $l = 30$. For moderate to low values of η_0, the results obtained with $l = 2$ show deviation of less than 4%. The table also shows the Central Processing Unit (CPU) times on an IBM 370/195 computer for all the five values of N_{cr}. For example, with $l = 2$, CPU time varies from 18 to 26 s. The CPU times increase disproportionately with increasing l. It may be pointed out that CPU times for a given value of η_0 are dependent on the value of N_{cr}. The CPU time increases as N_{cr} decreases. For $\eta_0 = 10$, with $l = 5$, the maximum deviation appears to be no more than 10% and in fact $l = 8$ produces a solution with very satisfactory accuracy for most engineering calculations. The benchmark values agreed with the finite-difference solution of Crosbie and Viskanta [6] to almost all the decimal places presented in the table.

For the case of pure radiation, i.e. $N_{cr} = 0$ for various values of optical thicknesses, the collocation solution was also compared with the exact analytical solution obtained by Heaslet and Warming [14]. These results for the temperature slips at the lower and upper walls are expressed in terms of nondimensional parameters α_0 and β_0, respectively, and, for the heat flux at the lower wall, are presented in Table 2. Since the boundary conditions (7) or (30) had to be dropped due to temperature slip at the walls, equation (29) with $N_{cr} = 0$, was also collocated at $\eta = 0$ and $\eta = \eta_0$ to supply the two additional equations. These two equations together with equation (32) with $N_{cr} = 0$, furnished the required set to obtain all the n unknown expansion coefficients. In these runs l was varied from a value of 2 to 10 which gave a corresponding variation in CPU from 91 to 855 s for all 12 cases of optical thickness $\eta_0 = 0.1$–3.0. The maximum error with $l = 2$ for the value of α_0 appears to be no more than 0.2%, for values of β_0 no more than 1.5%, and no more than 1% for the heat flux at $\eta_0 = 3.0$. Even for the case of a relatively optically thick medium with $\eta_0 = 10$ and $N_{cr} = 0$, the collocation method with $l = 2$ produces an answer with a deviation less than 7%, as can be seen from Table 1.

CONCLUDING REMARKS

The collocation method based on the use of piecewise polynomials combined with the use of the Gaussian–Legendre quadrature points as collocation points provides a very convenient technique for the solution of radiation–conduction problems. For the solution of these problems with the collocation method, one needs no more than standard proven software available at any computing laboratory and this considerably reduces the preparation time for successfully setting up the problem on the computer. By virtue of being a high order and noniterative method, it provides the means for obtaining the desired accuracy with a small number of equations at a reasonable computational cost.

Acknowledgement – This work was performed under the auspices of the U.S. Department of Energy.

REFERENCES

1. S. H. Chan and M. A. Grolmes, Hydrodynamically-controlled rewetting, *Nucl. Engng Design* **34**, 307–316 (1975).
2. S. H. Chan, D. W. Condiff and M. A. Grolmes, Radiative cooling of a voided subassembly, Argonne National Laboratory Report ANL-76-5 (1976).
3. D. H. Cho and S. H. Chan, Transient energy transfer by conduction and radiation for a sudden contact between molten UO_2 and sodium, Argonne National Laboratory Report ANL-78-34 (1978).
4. R. Viskanta and R. J. Grosh, Heat transfer by simultaneous conduction and radiation in an absorbing medium, *Trans. ASME, J. Heat Transfer* **C84**, 63–72 (1962).
5. R. Viskanta and R. J. Grosh, Effect of surface emissivity on heat transfer by simultaneous conduction and radiation, *Int. J. Heat Mass Transfer* **5**, 729–734 (1962).
6. A. L. Crosbie and R. Viskanta, Interaction of heat transfer by conduction and radiation in a nongray planar medium, *Wärme- und Stoffübertragung* **4**, 205–212 (1971).
7. E. E. Anderson and R. Viskanta, Spectral and boundary effects on coupled conduction–radiation heat transfer through semitransparent solids, *Warme- und Stoffubertragung* **6**, 14–24 (1973).
8. W. Lick, Energy transfer by radiation and conduction, in *Proc. 1963 Heat Transfer and Fluid Mechanics Institute*, pp. 14–26. Stanford University Press, Palo Alto, Calif. (1963).
9. D. H. Timmons and J. O. Mingle, Simultaneous radiation and conduction with specular reflection, IAAA 6th Aerospace Sciences Meeting, Paper No. 68–28, New York (1968).
10. C. C. Lii and M. N. Ozisik, Transient radiation and conduction in an absorbing, emitting, scattering slab with reflective boundaries, *Int. J. Heat Mass Transfer* **15**, 1175–1179 (1972).
11. E. E. Anderson and R. Viskanta, Effective conductivity for conductive–radiation by Taylor series expansion, *Int. J. Heat Mass Transfer* **14**, 1216–1220 (1971).
12. R. Viskanta and E. E. Anderson, Heat transfer in semitransparent solids, *Adv. Heat Transfer* **11**, 317–441 (1975).
13. A. L. Crosbie and R. Viskanta, Effect of band or line shape on the radiative transfer in a nongray planar medium, *J. Quant. Spectrosc. Radiat. Transfer.* **11**, 487–409 (1970).
14. M. A. Heaslet and R. F. Warming, Radiative transport and wall temperature slip in an absorbing planar medium, *Int. J. Heat Mass Transfer* **8**, 979–994 (1965).
15. J. T. Kriese and C. E. Siewert, Radiative transfer in a conservative finite slab with an internal source, *Int. J. Heat Mass Transfer* **13**, 1349–1357 (1970).
16. P. B. Kunasz and D. G. Hummer, Radiative transfer in spherically symmetric systems—III, *Mon. Not. R. astr. Soc.* **116**, 19–55 (1974).
17. J. Douglas and T. Dupont, A finite element collocation

method for quasi-linear parabolic equations, *Math. Comp.* **27**, 17–23 (1973).
18. C. De Boor and B. Swartz, Collocation at Gaussian points, *SIAM J., Numer. Anal.* **10**, 582–606 (1973).
19. L. Auer, An Hermitian method for the solution of radiative transfer problems, *J. Quant. Spectrosc. Radiat. Transfer* **16**, 931–937 (1976).
20. E. M. Sparrow and R. D. Cess, *Radiation Heat Transfer*, p. 256. Hemisphere Publishing Corporation (1978).
21. T. C. Chawla, G. Leaf and W. Chen, A collocation method using B-splines for one-dimensional heat or mass-transfer-controlled moving boundary problems, *Nucl. Engng Design* **35**, 163–180 (1975).
22. C. De Boor, Package for calculating with B-splines, *SIAM J. Numer. Anal.* **14**, 441–472 (1977).
23. K. E. Hillstrom, Nonlinear optimization routines in AMDLIB, Argonne National Laboratory, Applied Mathematics Division, TM-297 (1976).
24. M. J. D. Powell, A hybrid method of nonlinear equations, in *Numerical Methods for Nonlinear Algebraic Equations*, edited by P. Rabinowitz, pp. 87–114. Gordon & Breach, London (1970).
25. C. De Boor, CADR^r an algorithm for numerical quadrature, in *Mathematical Software*, edited by J. R. Rice. Academic Press, New York (1971).
26. T. C. Chawla, G. Leaf, W. L. Chen and M. A. Grolmes, The application of the collocation method using hermite cubic splines to nonlinear transient one-dimensional heat conduction problems, *Trans. ASME, J. Heat Transfer* **97**, 962–569 (1975).
27. W. J. Cody and H. C. Thacher, Jr., Rational Chebyshev approximations for the exponential integral $E_1(x)$, *Math. Comp.* **22**, 641–649 (1968).

RESOLUTION DES PROBLEMES DE RAYONNEMENT-CONDUCTION A L'AIDE D'UNE METHODE DE COLLOCATION UTILISANT UNE APPROXIMATION PAR LES FONCTIONS B-SPLINES

Résumé — Une méthode de collocation utilisant les fonctions B-splines et une quadrature de Gauss est introduite pour la première fois dans la résolution des problèmes de thermique avec couplage entre conduction et rayonnement. On montre que cette méthode fournit une technique sans itération qui, à partir d'un petit nombre d'équations, conduit à des solutions aussi précises que la méthode aux différences finies et ceci avec un coût de calcul raisonable. Par comparaison avec la solution analytique exacte dans le cas du rayonnement pur, on montre que six équations au plus permettent d'obtenir une précision supérieure à 2 %. Cette méthode parait être très intéressante dans la résolution des problèmes de conduction–rayonnement.

DIE LÖSUNG VON WÄRMELEITUNGSPROBLEMEN BEI STRAHLUNG DURCH EINE KOLLOKATIONSMETHODE MIT APPROXIMATION DURCH B-SPLINE-FUNKTIONEN

Zusammenfassung—Zum ersten Mal wird eine Kollokationsmethode, bei der B-Spline-Funktionen zur Approximation und die Punkte der Gaußschen Quadratur als Kollokations-Punkte verwendet werden, auf die Lösung von Wärmeübertragungsproblemen angewandt, die gleichzeitig von Leitung und Strahlung bestimmt sind. Es wird demonstriert, daß diese nichtiterative Methode mit einer nur geringen Zahl von Gleichungen ebenso genaue Lösungen wie die Methode der finiten Differenzen bei sehr annehmbarem Rechenaufwand liefern kann. Durch Vergleich mit exakten analytischen Lösungen für den Fall reiner Strahlung wird gezeigt, daß man bis zu mittleren Werten der optischen Dicke nicht mehr als 6 Gleichungen lösen muß, um eine Genauigkeit von besser als 2% zu erreichen. Unter diesen Umständen erscheint die Methode eine attraktive Möglichkeit für die Lösung von Strahlungs–Wärmeleitproblemen zu sein, wie sie bei Untersuchungen des Kernschmelzens von mit flüssigem Metall gekühlten schnellen Brutreaktoren (LMFBR) auftreten.

РЕШЕНИЕ ЗАДАЧ ПО ОДНОВРЕМЕННЫМ ИЗЛУЧЕНИЮ И ТЕПЛОПРОВОДНОСТИ МЕТОДОМ КОЛЛОКАЦИЙ С ИСПОЛЬЗОВАНИЕМ В-СПЛАЙНОВ В КАЧЕСТВЕ АППРОКСИМИРУЮЩИХ ФУНКЦИЙ

Аннотация — Метод коллокаций, основанный на использовании В-сплайнов в качестве аппроксимирующих функций и точек гауссовой квадратуры в качестве коллокационных точек, впервые используется для решения задач переноса тепла одновременно излучением и теплопроводностью. Показано, что этот метод, использующий переменную неитерационную схему счёта, позволяет только при небольшом количестве уравнений получить такую же точность решения, как и методом конечных разностей, но при меньших вычислительных затратах. Сравнение с точным аналитическим решением для случая только одного излучения показало, что вплоть до умеренных значений оптической толщины для получения точности в 2 % достаточно шести уравнений. Метод можно использовать при решении таких задач по излучению и теплопроводности, которые встречаются в случае плавления сердечников в результате пробоя.